Analysis of Canonical Molecular Orbitals to Identify Fermi Contact Coupling Pathways. 1. Through-Space Transmission by Overlap of P-31 Lone Pairs

ARTICLE *in* THE JOURNAL OF PHYSICAL CHEMISTRY A · NOVEMBER 2009

Impact Factor: 2.69 · DOI: 10.1021/jp908970f · Source: PubMed

Analysis of Canonical Molecular Orbitals to Identify Fermi Contact Coupling Pathways. 1. Through-Space Transmission by Overlap of ^{31}P Lone Pairs

Rubén H. Contreras,[†] Gustavo Gotelli,[‡] Lucas C. Ducati,[§] Thais M. Barbosa,[§] and Cláudio F. Tormena*[,§]

Department of Physics, FCEyN, University of Buenos Aires, and CONICET, Buenos Aires, Argentina, Department of Pharmaceutical Technology, FFyB, University of Buenos Aires, Buenos Aires, Argentina, and Organic Chemistry Department, Chemistry Institute, University of Campinas, P.O. Box 6154, 13084-971 Campinas, São Paulo, Brazil

Received: September 16, 2009; Revised Manuscript Received: October 29, 2009

In this work, a new approach to studying coupling pathways for the Fermi contact term of NMR spin−spin coupling constants (SSCCs) is presented. It is based on the known form of propagating the Fermi hole through a canonical molecular orbital (CMO). It requires having an adequate spatial description of the relevant canonical molecular orbitals, which are obtained by expanding CMOs in terms of natural bond orbitals (NBOs). For detecting the relevant contributions of CMOs to a given Fermi contact (FC) pathway, the description of the FC in terms of the triplet polarization propagator (PP) is used. To appreciate the potential of this approach, dubbed FCCP-CMO (Fermi contact coupling pathways-CMO), it is applied to analyze the through-space transmission of the FC term of J_{PP} SSCCs by overlap of the P lone pairs. This method can be applied using well-known quantum chemistry software without any further modification, which makes it appealing for use as a complement to SSCC measurements by NMR spectroscopy.

1. Introduction

Nuclear spin−spin coupling constants (SSCCs) measured in an isotropic phase by high-resolution NMR spectroscopy were rationalized by Ramsey[1] using a nonrelativistic formulation as originating in four different terms, namely, Fermi contact (FC), spin−dipolar (SD), paramagnetic spin−orbit (PSO), and diamagnetic spin−orbit (DSO)

$$^{n}J_{XY} = {}^{FC}J_{XY} + {}^{SD}J_{XY} + {}^{PSO}J_{XY} + {}^{DSO}J_{XY} \qquad (1)$$

where X and Y stand for the coupling nuclei and n is the number of bonds separating them.

During recent years, attention has been paid to the transmission mechanism of the FC interaction through molecular electronic structures, and its relationship with the behavior of the "Fermi hole" has been discussed.[2] Now, it is known that electron delocalization interactions are the main vehicle for transmitting the FC term for long-range SSCCs, $^{n}J_{XY}$ for $n > 3$.[3] Recently, several unusual coupling pathways for the FC contribution were reported,[4] where their rationalization was based on the analysis of charge-transfer interactions as studied by Weinhold et al.'s approach, natural bond orbitals (NBOs).[5] Those examples, as well as many others taken from the current literature, indicate that a method for easily detecting Fermi contact coupling pathways (FCCPs) is missing in the current literature.

In the present work, we report an approach, dubbed Fermi contact coupling pathway-canonical molecular orbital (FCCP-CMO), to provide such a method, and it can be applied using well-known quantum chemistry software without any further modification. It provides a qualitative analysis for different FCCPs resorting only to some physicochemical considerations. To implement this approach, the analytical expression for the FC term of SSCCs in terms of the polarization propagator (PP) approach is scrutinized from a physical point of view to understand the roles played by different canonical molecular orbitals (CMOs) in its transmission. Recall that exchange interactions make the Fermi hole span the whole region occupied by a CMO, and therefore, if knowledge is obtained about the spatial electronic distribution of a CMO within a molecule, then its role played in building up a given SSCC can be estimated qualitatively. For this reason, the two main clues to this new approach are (i) the comprehension, through PP inspection, of the roles played by different CMOs in transmitting the FC interaction and (ii) the expansion of CMOs in terms of NBOs as given by Weinhold et al.'s NBO 5.0 program.[6] As examples of the versatility of this approach three cases where the FC term of J_{PP} couplings for two proximate three-coordinate P atoms whose lone pairs overlap to some extent are considered in this work. The first example (Figure 1), taken as a test case, consists of *cis*-$H_2PC(H)=(H)CPH_2$, **1**, where the through-space transmission of the FC term of the $^{3}J_{PP}$ SSCC by overlap of the lone pairs was studied[7] using both the IPPP (inner projections of the polarization propagator) method[8] and Malkina et al.'s CED (coupling energy density) approach.[9] The second example (Figure 1) refers to the geminal $^{2}J_{PP}$ SSCCs in compounds of type $F_2P-X-PF_2$ (**2**), where X is a chalcogen atom, and this new approach is applied to the X = O and X = S cases. Some calculations intending to better understand such FCCPs are also discussed for the latter two compounds, X = O (**2a**) and X = S (**2b**).

The chosen examples take into account that it is well-known that a complex fragment containing a metal and two phosphorus nuclei offers the possibility of easily investigating the products by ^{31}P NMR spectroscopy determining the $^{2}J_{PP}$ coupling.[10,11] A linear correlation between experimental through-space-transmit-

* Corresponding author. E-mail: tormena@iqm.unicamp.br.
[†] FCEyN, University of Buenos Aires, and CONICET.
[‡] FFyB, University of Buenos Aires.
[§] University of Campinas.

10.1021/jp908970f
Published on Web 11/20/2009

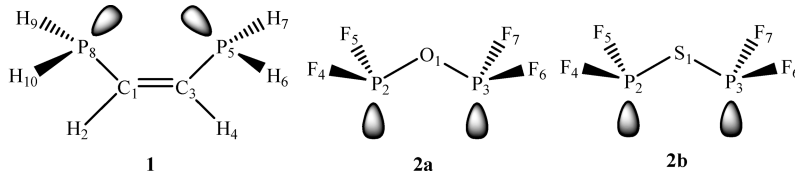

Figure 1. Structures of the studied compounds.

ted J_{PP} SSCCs and the P···P distance for ferrocenyl tetraphosphine coordination complexes has recently been observed.[12] There are also many compounds with structures similar to those of **2a** and **2b**, where large values of J_{PP} SSCCs suggest that the two P lone pairs overlap.[13] In this context, it is important to analyze the performance of this new approach to rationalize the transmission mechanisms for J_{PP} SSCCs. It is also well-established that the overlap between two proximate moieties leads to an efficient through-space mechanism for FCCPs, which takes place regardless of whether there is an attractive or repulsive interaction between the two coupling atoms.[14] In short, it seems interesting to present this approach for studying FCCPs with the examples quoted above to describe in detail the main features of some peculiar J_{PP} SSCCs in those model compounds that have shown unusual behavior for either their $^3J_{PP}$ or $^2J_{PP}$ SSCC.

2. Identifying the Role Played by Each CMO for Transmitting the FC Term in $^nJ(X,Y)$

In this simple method for analyzing FCCPs, it is important to identify CMOs that are relevant for transmitting the FC interaction corresponding to a given $^nJ(X,Y)$ SSCC. This can be achieved by resorting to the polarization propagator (PP) formalism, where the FC term can be written as in eq 1 and can be decomposed into contributions from molecular orbitals (MOs), as shown in eq 2, where n is the number of chemical bonds separating the X and Y coupling nuclei, i and j are occupied MOs, and a and b are vacant MOs. Each term of eq 2 can be written as in eq 3[15]

$$^nJ^{FC}_{XY} = \sum_{ia,jb} {}^nJ^{FC}_{ia,jb}(XY) \tag{2}$$

$$^nJ^{FC}_{ia,jb}(XY) = {}^3W_{ia,jb}(U^{FC}_{ia,X}U^{FC}_{jb,Y} + U^{FC}_{ia,Y}U^{FC}_{jb,X}) \tag{3}$$

In eq 3, $U_{ia,C}$ ($U_{jb,H}$) are the "perturbators", that is, the matrix elements $U^{FC}_{ia,X} = \langle i|\delta(\vec{r}_X)|a\rangle$ of the FC operator between the occupied i (j) and vacant a (b) MOs evaluated at the X (Y) site of the coupling nuclei, and they constitute a measure of the strength of the $i \rightarrow a$ ($j \rightarrow b$) virtual excitation due to that operator. In addition

$$^3W_{ia,jb} = ({}^3A - {}^3B)^{-1}_{ia,jb} \tag{4}$$

represents the elements of the triplet PP matrix, where

$$^3A_{ia,jb} = (\varepsilon_a - \varepsilon_i)\delta_{ab}\delta_{ij} - \langle aj|bi\rangle \tag{5}$$

and

$$^3B_{ia,jb} = \langle ab|ji\rangle \tag{6}$$

When using localized molecular orbitals (LMOs), eqs 2−6 correspond to the CLOPPA method (contributions from localized orbitals within the polarization propagator approach), first developed for semiempirical approaches[15b] but later also implemented using ab initio wave functions.[16] During the past few years, similar expressions have been extended to be used with Kohn−Sham[17] localized orbitals by Cremer et al.[18] and Sauer et al.[19]

Qualitative analyses similar to that presented here, FCCP-CMO, were carried out previously for eqs 2−6 introducing several approximations considering that virtual orbitals can be assumed to behave like NBO antibonding orbitals whereas occupied orbitals behave like either bonding NBOs or NBO lone pairs.[20] Such an approach was employed to rationalize how hyperconjugative interactions affect $^1J_{CH}$ SSCCs. However, when intending to use it to rationalize longer-range SSCCs, this methodology becomes rather cumbersome, although it is known that, in most cases, the FC contribution to long-range SSCCs is transmitted by electron delocalization interactions.[21] In this work, eqs 2−6 are used only to appreciate which CMOs are significant for transmitting a given FCCP. The term $^nJ^{FC}_{ia,jb}(XY)$ (eq 3) is called here an FCCP. In particular, FCCPs determined by the overlap between lone pairs of two P atoms that are proximate in space are sought. Each FCCP depends both on the $^3W_{ia,jb}$ matrix element and the perturbators. It is known[15a] that the former are largest for "diagonal" matrix elements (i.e., those for which $i = j$ and $a = b$) and the latter are important whenever there is a substantial overlap between $i = j$ and $a = b$ at the positions of both coupling nuclei. Referring only to diagonal elements of the PP matrix, a pair of occupied and vacant CMOs defining an efficient FCCP can be spotted by observing their respective NBO expansions. In fact, for being efficient, the occupied CMO should be made up of bonds or lone pairs containing the coupling nuclei, and the unoccupied CMO should be made up of antibonding orbitals containing the coupling nuclei. It must also be recalled that, according to eqs 4−6, only the diagonal $^3W_{ia,jb}$ matrix elements depend explicitly on the virtual-occupied energy gap, $\Delta_{a,i} = (\varepsilon_a - \varepsilon_i)$. That dependence is such that the smaller the energy gap, the larger the contribution to the respective FCCP. With these ideas in mind, it is quite easy to identify the CMOs that constitute efficient FCCPs for a given SSCC.

It is highlighted that actual calculations of eqs 2−6 are not carried out in this work within either ab initio or DFT frameworks. However, total SSCC calculations are carried out within CP-DFT (coupled perturbed-density functional theory) as implemented in the Gaussian 03 suite of programs.[22]

3. Computational Details

All structures were fully optimized at the MP2[23] and aug-cc-pVTZ basis set[24] level using the Gaussian 03[22] program. Electronic structures were studied using NBO analyses using the B3LYP[25] hybrid functional and IGLO-III[26] basis set with the optimized geometries.

J_{PP} couplings in compounds **1**, **2a**, and **2b** were calculated using the CP-DFT/B3LYP methodology[27] as implemented in the Gaussian 03 package[22] of programs. All four terms of $^2J_{PP}$ SSCCs for compounds **2a** and **2b** (FC, SD, PSO, and DSO) were calculated using the pcJ-4 basis set,[28] which was developed for SSCCs calculation within the DFT-B3LYP framework for

phosphorus atoms. Some SSCC calculations were also carried out within the same framework but using the IGLO-III[26] basis set, which is less expensive than the pcJ-4 basis set. The cc-pVTZ basis set was applied for other atoms.

The CMO information needed to make the analysis of the FCCP by overlap of the P lone pairs in compounds **1**, **2a**, and **2b** was gathered directly from the NBO 5.0 program using the following keyword in the Gaussian 03 program input file: $nbo cmo $end. With this option, the NBO 5.0 program yields CMOs expanded in NBOs, along with the respective coefficients given in terms of the percent participation in each CMO and its energy.

4. Results and Discussion

4.a. Transmission of the FC Term by Overlap of ^{31}P Lone Pairs in Compound 1. To test this approach in a well-known case, the "through-space" (TS) transmission of the FC contribution to the $^3J_{PP}$ SSCC by overlap of the P lone pairs in **1** (Figure 1) is studied. The relevant diagonal term of the triplet PP matrix must be accompanied by an occupied CMO satisfying the following conditions to yield a non-negligible FCCP determined by the overlap of both P lone pairs: (a) An occupied CMO expanded in terms of NBOs must be contributed by both lone pairs, and the larger their coefficients, the more relevant their contributions to the FCCP defining the TS transmission. This condition must be satisfied to guarantee a significant s percent character at the site of the P coupling nuclei. (b) Analogously, virtual CMO*s in their expansion in NBOs must contain antibonding orbitals involving both P atoms. However, low-lying Rydberg orbitals localized on the P atoms could also be important. (c) When rotating a phosphine moiety around the C_3—P_5 bond, angle θ, from 0° to 90° (see Figure 1), each FCCP contributing to the lone-pair (LP) overlap should notably decrease. This means that such CMOs for the 90° conformation should show a much smaller coefficient for one or both NBOs representing the P lone pairs.

Virtual transitions involving the same occupied CMO but a different virtual one, CMO*, can also contribute to diagonal elements of the triplet PP matrix. Because the study of the TS transmission by overlap of both P lone pairs is sought, it is concluded that, in this case, the analysis of occupied CMOs is the most important point, and therefore, emphasis will be put on analyzing them.

Diagonal elements of the PP matrix, $^3W_{ia,ia}$, depend explicitly on the virtual−occupied energy gap, $\Delta_{a,i} = \varepsilon_a - \varepsilon_i$, in such a way that a smaller energy gap corresponds to a larger FCCP, provided that all other parameters are the same. Nonetheless, it must be recalled that all PP matrix elements depend on all occupied and vacant CMOs.

Two related questions are: To what extent do NBO coefficients for a given CMO depend on the basis set used in their calculations? How do NBO coefficients found to expand CMOs calculated within the DFT framework resemble those obtained within the Hartree−Fock approach (employing the same basis set)? To answer these two questions, CMOs in **1** were expanded in NBOs using the same geometry at these three different levels of theory, B3LYP/6-311++G(d,p), B3LYP/IGLO-III, and Hartree−Fock/6-311++G(d,p). Relevant occupied CMOs for describing the FCCP by overlap of P lone pairs were compared, and qualitatively, similar contributions were found in the three cases, as can be appreciated in the Supporting Information. This suggests that, in polyatomic compounds, particular FCCPs can be predicted qualitatively without resorting to computationally demanding SSCC calculations. It is recalled that compound **1** is unsaturated, and therefore, the FC term cannot be calculated within the CP-Hartree−Fock approach. Nonetheless, the analysis of CMOs is adequate to predict FCCPs for different SSCCs because this CMO analysis is not affected by nonsinglet instabilities of the ground state wave function.

TABLE 1: DFT-B3LYP $^3J_{PP}$ SSCCs (in Hz) Calculated in 1 Using the 6-311++G(d,p) and IGLO-III Basis Sets for Conformations $\theta = 0°$ and 90°

	6-311++G(d,p)		IGLO-III	
	$\theta = 0°$	$\theta = 90°$	$\theta = 0°$	$\theta = 90°$
FC	185.3	67.5	182.2	70.8
total	186.3	66.2	183.6	69.7

TABLE 2: Experimental $^3J_{PP}$ SSCCs (in Hz) taken from Ref 29 Showing That a Bulky *t*-Butyl Group Geminal to One of the Phosphino Groups Yields a Substantial Reduction of That Coupling, Commensurate with Differences Calculated for Such SSCCs Shown in Table 1

compound	$^3J_{PP}$
cis-$Ph_2PCH{=}C(Ph)PPh_2$	146
cis-$Ph_2PCH{=}C(t\text{-}Bu)PPh_2$	37
cis-$Ph_2PCH{=}C(Ph)PEtPh$	146
cis-$Ph_2PCH{=}C(t\text{-}Bu)PEtPh$	45

On the other hand, the $^3J_{PP}$ SSCC in **1** was calculated using the B3LYP/6-311++G(d,p) and B3LYP/IGLO-III approaches. The results thus found are listed in Table 1 for $\theta = 0°$ and 90° conformations. There are no experimental values for compound **1**; however, the trends shown in Table 1 are in agreement with experimental values for similar compounds reported in the literature.[29] In Table 2, a few experimental data reported by Carty et al.[29] are reproduced. It is observed that a bulky *t*-butyl group placed geminal to either the PPh_2 or PEtPh phosphino moieties introduces steric effects, forcing them to rotate around the P−C bond, decreasing the overlap of the P lone pairs and, concomitantly, decreasing the $^3J_{PP}$ SSCC.

Following comments made in section 2, CMOs defining FCCPs by overlap of the P lone pairs for the $\theta = 0°$ conformation should contain, simultaneously, both P lone pairs in their NBO expansions. Their relative importance can be appreciated from these considerations. They are larger for larger lone-pair coefficients in that expansion, and the corresponding energy gap, $\Delta = \varepsilon_a - \varepsilon_i$, is smaller. The respective virtual CMO*s should contain, simultaneously, in their expansion NBO antibonding orbitals involving both P atoms (although, in some cases, it could also be a low-lying Rydberg orbital localized on that atom). This analysis is restricted to diagonal terms of the triplet PP matrix elements because they yield the major contributions.

Table 3 includes, for conformation $\theta = 0°$, all occupied CMOs in **1** that contain both lone pairs in their expansions in terms of NBOs. Such values are also compared with their respective NBO expansions for $\theta = 90°$. It is recalled that a threshold of 5% NBO contribution to a given CMO is given in the output of the NBO 5.0 program; in addition, the CMOs are numbered according to the output of that program; that is, they are labeled from lowest to highest orbital energy. The NBO numbering is shown in square brackets. It is observed that NBO P lone-pair contributions to CMOs 14 and 15 change very little when going from the 0° to the 90° conformation. Therefore, they can hardly be considered to participate in the TS transmission involving the overlap of P lone pairs; probably, this is due to the low energies of these two CMOs. It is recalled that the squared coefficient gives the relative contribution of each NBO to a given CMO. In CMO 16, both NBO P lone pairs yield

TABLE 3: Comparison between Occupied CMOs Involving Both P Lone Pairs for $\theta = 0°$ and $\theta = 90°$ in Compound 1. Orbital Energies are in Hartrees and Numbers in Square Brackets Correspond to the Numbering of NBO Orbitals as Given by the NBO 5.0 Program

CMO	0°	90°
14	0.261*[24]: LP(P_8)	−0.274*[23]: LP(P_5)
	−0.261*[23]: LP(P_5)	0.270*[24]: LP(P_8)
ε(14)	−0.675984	−0.674582
15	0.320*[24]: LP(P_8)	0.319*[23]:LP(P_5)
	0.320*[23]: LP(P_5)	0.313*[24]: LP(P_8)
ε(15)	−0.628898	−0.630643
16	−0.227*[24]: LP(P_8)	—[a]
	0.227*[23]: LP(P_5)	—[a]
ε(16)	−0.523549	−0.527671
23	0.600*[24]: LP(P_8)	0.802*[24]: LP(P_8)
	0.600*[23]: LP(P_5)	—[a]
ε(23)	−0.284566	−0.267335
24	−0.591*[23]:LP(P_5)	0.655*[23]: LP(P_5)
	0.591*[24]: LP(P_8)	—[a]
ε(24)	−0.250928	−0.251334

[a] NBO contribution is below the threshold taken in this work, i.e., 5%.

significant contributions for the 0° conformation, but they are below the 5% threshold for the 90° conformation. On the other hand, CMOs 23 and 24 both contain significant contributions for the 0° conformation, and the contribution of one of the two lone pairs increases for the 90° conformation, whereas the other one is below the 5% threshold. Comparing the CMO orbital energies for data displayed in Table 3, it is observed that CMOs 23 and 24 define the main FCCPs involved in the P lone-pair overlap. It is noted that CMO 24 is the highest occupied molecular orbital (HOMO) for compound **1**. Of course, this does not mean that the HOMO plays an important role in the FCCPs for all SSCCs; that is, this is a peculiarity for this SSCC in this compound and not a general consideration.

Because CMOs 23 and 24 in **1** define the main FCCPs for transmitting the $^3J_{PP}$ SSCC through space via the P lone pairs, plots of these CMOs are displayed in Figure 2. These plots yield interesting visualizations of the role played by the ^{31}P lone pairs in transmitting such SSCCs.

The visualizations shown in Figure 2 could be misleading if they are intended to be used in a quantitative way, assuming that the FCCP involving CMO 23 is more efficient than that containing CMO 24. (It is assumed that, in both cases, the same virtual CMO* is involved in the FCCPs.) This problem occurs because these plots correspond to CMOs, and therefore, in both cases, any information associated with the FC interaction, the Fermi hole that is "leaked" into one of them, would span the whole CMO spatial region owing to exchange interactions originating in the Pauli exclusion principle.

The difference in energy between CMOs 23 and 24 can be rationalized by taking into account the fact that several contributions, less than 5% each, push down the energy of CMO 23. This difference determines different energy gaps for virtual transitions involving a given virtual CMO, as shown in Table 4, where the main virtual transitions defining the TS transmission by overlap of lone pairs for $\theta = 0°$ in **1** are displayed.

Which virtual orbitals are involved in each FCCP defining the TS transmission of the FC term by P lone-pair overlap for $^3J_{PP}$ SSCC in **1**? There are several, because most antibonding orbitals contain at least one of the P atoms (with the exception of the $\sigma^*_{C1=C3}$ and $\pi^*_{C1=C3}$ vinyl antibonding orbitals). In Table 4 are listed the energy gaps for the main virtual excitations involving occupied CMOs 23 and 24.

Obviously, occupied CMOs 16, 23, and 24 correspond to the overlap between the P_5 and P_8 lone pairs, in agreement with the results discussed by Malkina et al.[9] It is noted that contributions from CMOs 23 and 24 yield the largest part of the TS FC transmission because they show the largest contributions from the NBO lone pairs and their energy gaps are smaller than those for CMO 16 (see Table 4).

In Table 5 are listed the main NBO contributions to virtual CMO*s 27, 29, and 30. Their main contributions come from the σ^*_{CP} antibonding orbitals, whereas the second most important contributions correspond to σ^*_{PH} antibonding orbitals, with small contributions from Rydberg orbitals localized at a P atom. Virtual CMO* 30 corresponds to a different combination of σ^*_{CP} antibonding orbitals.

Analysis of different virtual CMO*s participating in all FCCPs requires the consideration of many virtual transitions involving a few occupied CMOs with many virtual CMO*s (depending on the basis set size). However, the virtual transitions included in Table 4 are the largest because all others imply larger energy gaps. It is important to note that most SSCC calculations in terms of LMOs carried out by the approaches of Cremer et al.[18] and Sauer et al.[19] show explicitly only the occupied LMOs. Similarly, with the present approach, the analysis of CMO contributions to eq 3 can be described by considering the occupied CMOs; for the present problem, they correspond to the overlap of the two P lone pairs.

This analysis of the TS transmission of a $^3J_{PP}$ SSCC corresponding to P atoms with overlapping lone pairs for a well-known case, namely, compound **1**,[9] shows that the present method, FCCP-CMO, is a versatile qualitative approach for easily identifying coupling pathways for the transmission of the FC term. For this reason, in the next subsection, this approach is applied to study a similar TS transmission for $^2J_{PP}$ SSCCs in compounds **2a** and **2b**.

4.b. FC Transmission by Overlap of ^{31}P Lone Pairs in Compounds 2a and 2b. The results discussed in section 4.a show, on one hand, that the approach presented in this work can describe correctly FC transmission through overlap of P lone pairs, discussed previously by Malkina et al.[9] using their CED approach to visualize it. On the other hand, it suggests that the strong temperature dependence of the $^2J_{PP}$ SSCC experimentally observed in **2b** originates in changes of the P lone-pair overlap. Since 1970, it has been known that the $^2J_{PP}$ SSCC in $F_2P-S-PF_2$ (**2b**) presents a large temperature dependence varying from 392.9 Hz at −120 °C to 274.1 Hz at 31 °C, which was rationalized as originating in changes of conformational equilibrium between the cis and trans conformations (Figure 1).[30] On the other hand, for the corresponding oxygen derivative (**2a**), the experimental $^2J_{PP}$ value is 10 Hz at 100 °C. To gain a deeper insight into this effect, the following studies are discussed.

Before applying the FCCP-CMO approach to **2a** and **2b**, several aspects of $^2J_{PP}$ SSCCs in $F_2P-X-PF2$ [X = O (**2a**) and S (**2b**)] are discussed. In Tables 6 and 7, the $^2J_{PP}$ SSCCs for compounds **2a** and **2b** calculated with the B3LYP functional using two different basis sets are displayed.

In Tables 6 and 7, one can see that the $^2J_{PP}$ SSCCs in **2a** and **2b** are mainly dominated by the FC contribution. Differences in the $^2J_{PP}$ SSCCs for the cis and trans conformations are notably larger for **2b** than for **2a**, probably because of the smaller P−S−P angle (93°) in **2b** than in **2a** (126°). This trend suggests that, for the cis conformation in both compounds, the overlap of the P lone pairs is efficient for transmitting TS the FC interaction. In Figure 3 are plotted $^2J_{PP}$ SSCCs as a function of

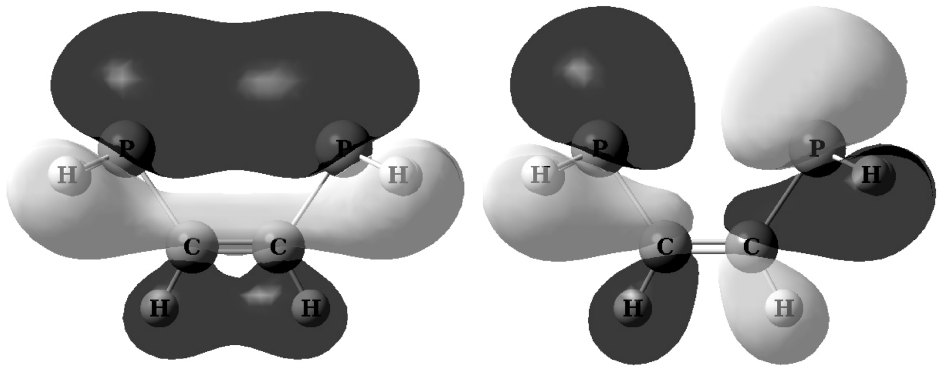

Figure 2. Plots of occupied CMOs 23 and 24 corresponding to the main FCCPs by the overlap of the two P lone pairs for the $^3J_{PP}$ SSCC in compound **1**.

TABLE 4: Energy Gaps for the Most Relevant Virtual Transitions, $(VT)_{a,i}$, Defining the TS FCCPs in 1[a]

$(VT)_{a,24}$	$\Delta(\varepsilon_a - \varepsilon_{24})$	$(VT)_{a,23}$	$\Delta(\varepsilon_a - \varepsilon_{23})$
27−24	0.254645	27−23	0.288283
29−24	0.255881	29−23	0.289519
30−24	0.270646	30−23	0.304284

[a] Energy gaps, $\Delta(\varepsilon_a - \varepsilon_i)$, are in hartrees ($a$ stands for CMO* 27, 29, or 30).

TABLE 5: Main NBO Contributions to Virtual Canonical MOs, CMO*, Involved in Virtual Transitions Listed in Table 4,a

CMO*	energy	main NBO contributions
27	0.003717	0.425*[142]: σ^*_{C3-P5} −0.425*[140]: σ^*_{C1-P8}
29	0.004953	0.392*[146]: σ^*_{P8-H10} 0.392*[144]: σ^*_{P5-H7} −0.390*[145]: σ^*_{P8-H9} −0.390*[143]: σ^*_{P5-H6} −0.264*[76]: Ry^*_{P5} 0.264*[109]: Ry^*_{P8}
30	0.019718	−0.355*[140]: σ^*_{C1-P8} −0.355*[142]: σ^*_{C3-P5}

[a] Orbital energies are in hartrees; Ry* stands for a Rydberg orbital.

the P−X−P angle in **2a** and **2b** for the cis and trans conformations. The results displayed in Figure 4 support the assumption about a strong contribution of the FC term to the $^2J_{PP}$ SSCC owing to the overlap of both P lone pairs.

In Figure 4, it is observed that, for **2b**, $\log(^2J_{PP})$ correlates linearly with the P···P distance. This straight line corresponds to an exponential decrease of the P−P lone-pair overlap as a function of the P···P distance, supporting the idea that the main contribution to the $^2J_{PP}$ SSCC versus the P−S−P bond angle dependence originates mainly in the overlap of P−P lone pairs.

The P lone-pair overlap in **2b** was also modified by changing the bond length of one of the S−P bonds. Results for the cis and trans conformers are displayed in Figure 5. It is clearly observed that the sensitivity of $^2J_{PP}$ for the cis conformer is notably higher than that for the trans conformer.

The results displayed in Figures 3−5 strongly support the idea that the P lone-pair overlap is the main $^2J_{PP}$ transmission mechanism for the cis conformers of **2a** and **2b**. Therefore, both compounds are considered to be interesting examples for further testing of the performance of the FCCP-CMO approach for the study of FC coupling pathways. To this end, two conformations are considered for **2a** and **2b**, namely, the 0° and 90°

TABLE 6: Calculation of $^2J_{PP}$ SSCCs for Cis and Trans Conformers of 2a[a]

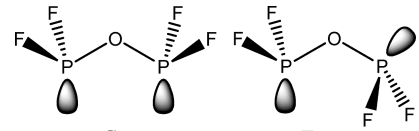

Cis *Trans*

	B3LYP/pcJ-4		B3LYP/IGLO-III	
	cis	trans	cis	trans
FC	215.7	−13.7	193.2	−16.9
SD	0.3	0.7	0.3	0.7
PSO	−1.8	3.0	−2.0	2.8
DSO	0.0	0.0	0.0	0.0
total	214.2	−10.0	191.6	−13.4

[a] Geometries were optimized at the MP2/aug-cc-pVTZ level, and all isotropic contributions to $^2J_{PP}$ were calculated within the DFT-B3LYP approach using pcJ-4 and IGLO-III basis sets.

TABLE 7: Calculation of $^2J_{PP}$ SSCCs for 2b Cis and Trans Conformers[a]

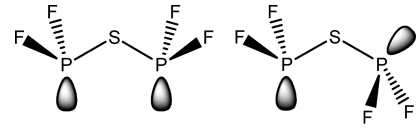

Cis *Trans*

	B3LYP/pcJ-4		B3LYP/IGLO-III	
	cis	trans	cis	trans
FC	621.3	−13.8	596.9	−13.2
SD	−0.7	−1.0	−0.7	−1.0
PSO	−0.4	−0.9	−0.5	−1.1
DSO	0.0	0.0	0.2	0.0
total	620.3	−15.7	595.9	−15.1

[a] Geometries were optimized at the MP2/aug-cc-pVTZ level, and all isotropic contributions to $^2J_{PP}$ were calculated within the DFT-B3LYP approach using pcJ-4 and IGLO-III basis sets.

conformations. The first is the cis conformation shown in Figure 1, and the second is obtained from the 0° conformation by rotating a PF_2 group by 90° around the respective X−P bond with X = O in **2a** and X = S in **2b**. In Tables 8 and 9 are listed the expansions of relevant occupied CMOs in terms of NBOs for compounds **2a** and **2b**, respectively. As noted above for **1**, for the 0° conformation, only CMOs containing simultaneously both LPs are relevant for transmitting the FC term through the overlap of P lone pairs. The respective CMO orbital energies are also displayed. The effects of different basis sets in relevant occupied CMOs for describing the FCCP by the overlap of P

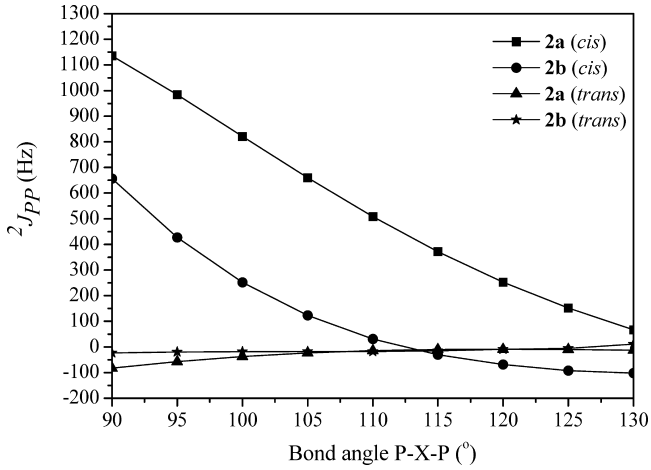

Figure 3. Dependence of $^2J_{PP}$ SSCC on bond angle (P−X−P) variation, for cis and trans conformations of compounds 2**a** (X = O) and **2b** (X = S).

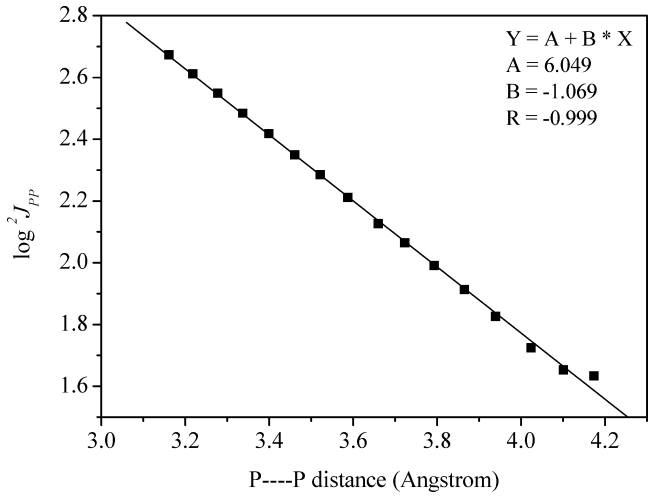

Figure 4. Linear correlation between log $^2J_{PP}$ and P···P distance when changing the P−S−P angle for the **2b** cis conformer.

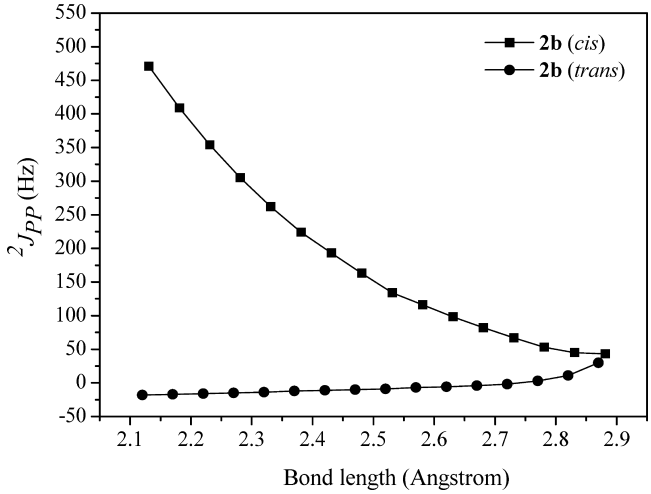

Figure 5. $^2J_{PP}$ SSCC vs one of the S−P bond-lengths in **2b**.

lone pairs were compared, and qualitatively, similar contributions were found in the four cases, as can be appreciated from the Supporting Information.

The similarities between the data listed in Tables 3, 8, and 9 are striking. P lone-pair contributions to the two lowest (in energy) CMOs are only very slightly different for the 0° and 90° conformations. For this reason, these CMOs are not considered as contributing to the TS transmission by the P lone-pair overlap. The CMOs that are next higher in energy (CMO 16 in Table 3, CMOs 26 and 27 in Table 8, and CMOs 30 and 37 in Table 9) correspond to the sought TS FCCPs because, for the 90° conformation, they are made up by at most one lone pair (of course, within the threshold limit). However, it can be predicted that such contributions are not very significant because

TABLE 8: Expansion of Occupied CMOs in Terms of NBOs in 2a Containing Simultaneously Both P Lone Pairs for the 0° Conformation,[a] Compared with the NBO Expansion for the Same Orbitals for the θ = 90° Conformation[b]

CMO	0°	90°
21	−0.272*[25]: LP(P_3)	0.294*[25]: LP(P_2)
	0.272*[24]: LP(P_2)	−0.269*[24]: LP(P_3)
ε(21)	−0.730283	−0.729072
22	0.302*[25]: LP(P_3)	0.296*[24]: LP(P_2)
	0.302*[24]: LP(P_2)	0.284*[25]: LP(P_3)
ε(22)	−0.646726	−0.647244
26	0.283*[25]: LP(P_3)	−0.304*[25]: LP(P_3)
	0.283*[24]: LP(P_2)	−[c]
ε(26)	−0.534330	−0.522738
27	−0.236*[25]: LP(P_3)	0.284*[24]: LP(P_2)
	0.236*[24]: LP(P_2)	−[c]
ε(27)	−0.511662	−0.521829
36	−0.569*[25]: LP(P_3)	0.713*[25]: LP(P_3)
	0.569*[24]: LP(P_2)	0.254*[24]: LP(P_2)
ε(36)	−0.340868	−0.337163
37	0.533*[25]: LP(P_3)	0.533*[24]: LP(P_2)
	0.735*[24]: LP(P_2)	0.283*[25]: LP(P_3)
ε(37)	−0.327815	−0.329827

[a] Only such contributions are included, Figure 1. [b] NBOs are numbered (in square brackets) as given by the NBO program. [c] NBO contribution is below the threshold taken in this work, i.e., 5%.

TABLE 9: Expansion of Occupied CMOs in Terms of NBOs in 2b Containing Simultaneously Both P Lone Pairs for the 0° Conformation,[a] Compared with the NBO Expansion for the Same Orbitals for the θ = 90° Conformation[b]

CMO	0°	90°
25	0.329*[28]: LP(P_2)	0.355*[29]: LP(P_3)
	−0.329*[29]: LP(P_3)	−0.328*[28]: LP(P_2)
ε(25)	−0.680020	−0.680653
26	0.257*[28]: LP(P_2)	0.264*[28]: LP(P_2)
	0.257*[29]: LP(P_3)	0.225*[29]: LP(P_3)
ε(26)	−0.640269	−0.638896
30	0.264*[28]: LP(P_2)	−0.236*[29]: LP(P_3)
	0.264*[29]:LP(P_3)	−[c]
ε(30)	−0.521630	−0.519269
37	−0.301*[28]: LP(P_2)	0.364*s [29]: LP(P_3)
	−0.301*[29]: LP(P_3)	−[c]
ε(37)	−0.442572	−0.436690
38	0.293*[28]: LP(P_2)	0.355*[28]: LP(P_2)
	−0.293*[29]: LP(P_3)	0.232*[29]: LP(P_3)
ε(38)	−0.455572	−0.420811
39	0.489*[28]: LP(P_2)	0.485*[29]: LP(P_3)
	−0.489*[29]: LP(P_3)	−[c]
ε(39)	−0.313003	−0.319199
41	0.450*[28]: LP(P_2)	0.450*[29]: LP(P_3)
	0.450*[29]: LP(P_3)	−[c]
ε(41)	−0.300842	−0.291817

[a] Only such contributions are shown, Figure 1. [b] NBOs are numbered (in square brackets) as given by the NBO program. [c] NBO contribution is below the threshold taken in this work, i.e., 5%.

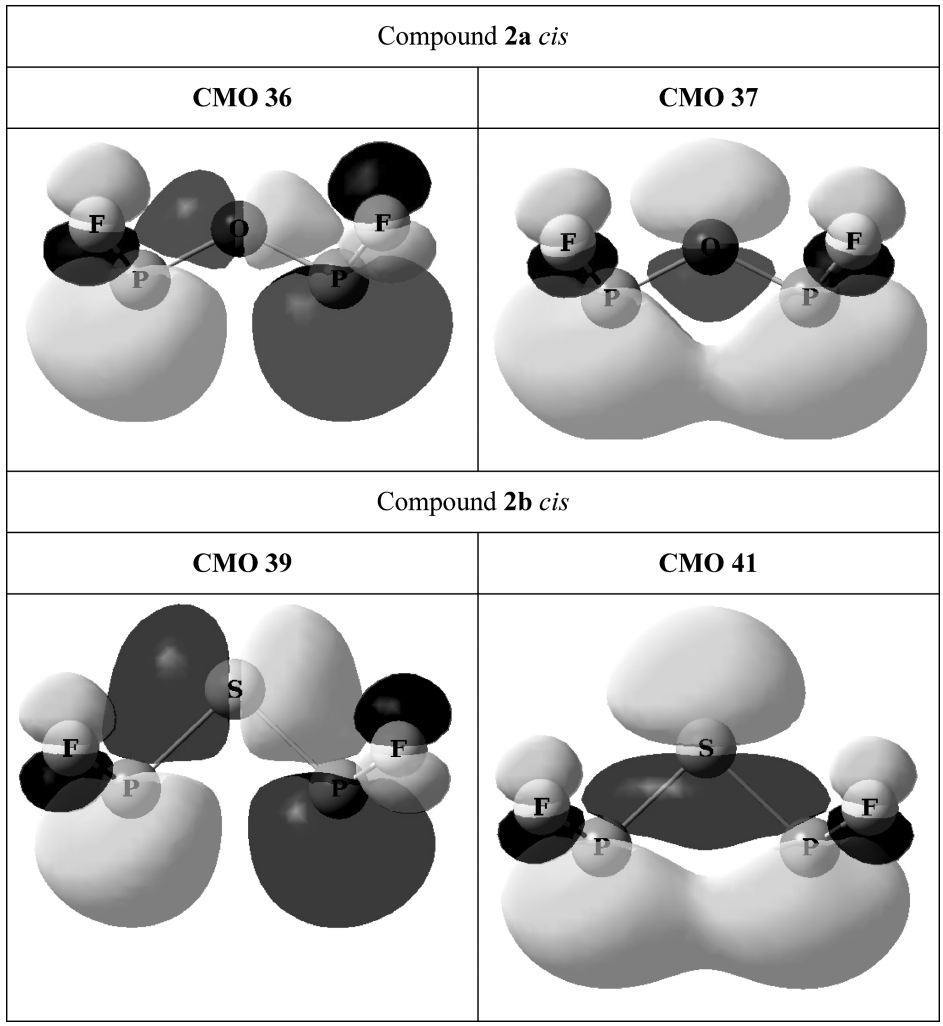

Figure 6. Plots of CMOs 36 and 37 in **2a** and 39 and 41 in **2b** calculated at the B3LYP/IGLO-III level. In each compound, these CMOs yield the two largest contributions to the TS transmission of the FC by P lone-pair overlap.

the lone-pair contributions have small coefficients and such CMOs are low in energy, defining large virtual−occupied energy gaps. Obviously, the largest contributions to the lone-pair overlap transmission originate in CMOs 23 and 24 in **1**, CMOs 36 and 37 in **2a**, and CMOs 39 and 41 in **2b**. The small differences observed in the TS transmission between the $^3J_{PP}$ SSCC in **1** and the $^2J_{PP}$ SSCCs in **2a** and **2b** originate in interactions of the type $LP_2(X) \rightarrow (P_1{-}F)^*$ that, for the 0° conformation, define an additional coupling pathway of the type $(P_2{-}F)^* \leftarrow LP_2 \rightarrow (P_1{-}F)^*$, where LP_2 stands for the chalcogen lone pair perpendicular to the P−X−P plane.

In Figure 6 are plotted CMOs 36 and 37 in **2a** and CMOs 39 and 41 in **2b**. Again, these plots show the interesting performance of the FCCP-CMO approach for visualizing the most important coupling pathways for the FC term of the $^2J_{PP}$ SSCCs in **2a** and **2b**. Comments similar to those made with respect to Figure 2 are relevant also for the visual representations presented in Figure 6.

As noted above, for the purposes of this work, it is not relevant to discuss the role played by virtual CMO*s defining each FCCP. It is emphasized that each relevant occupied CMO defines many diagonal terms of the PP matrix; however, their relative importance decreases with increasing virtual−occupied energy gap. From a qualitative point of view, in many cases, it is expected that few FCCPs can provide important information on the electronic molecular structure of the compound under study.

Concluding Remarks

In this work, a novel practical approach for identifying coupling pathways for the FC term of SSCCs is presented. It is based on an analysis of the spatial distribution of canonical molecular orbitals (CMOs) that satisfy the Pauli exclusion principle, and therefore, the Fermi hole is propagated through the whole region spanned by each CMO through exchange interactions. The spatial extent of each CMO is studied by expanding it in terms of NBOs as given by the NBO 5.0 program. For this reason, this approach is dubbed FCCP-CMO, Fermi contact coupling pathways in terms of canonical molecular orbitals, and each CMO can be graphically visualized, giving an intuitive and useful picture. It is expected that the FCCP-CMO method will be useful as a complementary tool to high-resolution NMR spectroscopic measurements for increasing insight into electronic molecular structure when rationalizing SSCCs largely dominated by the FC term. As practical examples of the FCCP-CMO approach, this work includes analyses of the through-space transmission of the FC term by the overlap of lone pairs of two three-coordinated P atoms that are proximate in space. **1**, **2a**, and **2b** were taken as model systems to carry out such analyses. Different examples will be presented in forthcoming articles.

It is emphasized that the realization of these analyses requires only very well-known quantum chemical software without any further modification. Moreover, the rather involved theoretical

principles governing the Fermi contact interaction are resumed in a few practical rules for easily identifying canonical molecular orbitals that should be relevant for transmitting the FC term for a given SSCC.

Acknowledgment. R.H.C. gratefully acknowledges financial support from CONICET (Grant 5119/05) and UBACYT (Grant X-047). C.F.T. is grateful to FAPESP (Grant 06/03980-2, 08/06282-0) for financial support of this work and a scholarship to L.C.D. and also to CNPq for a scholarship to T.M.B. and fellowships to C.F.T.

Supporting Information Available: Comparison of NBO contributions to occupied CMOs in *cis*-$H_2PCH{=}HCPH_2$ for the 0° conformation and CMO analyses for compounds **2a** and **2b** obtained by applying the B3LYP hybrid functional and different basis sets. This material is available free of charge via the Internet at http://pubs.acs.org.

References and Notes

(1) Ramsey, N. F. *Phys. Rev.* **1953**, *91*, 303.

(2) (a) Soncini, A.; Lazzeretti, P. *J. Chem. Phys.* **2003**, *119*, 1343. (b) Castillo, N.; Matta, C. F.; Boyd, R. J. *J. Chem. Inf. Model.* **2005**, *45*, 354.

(3) Contreras, R. H.; Esteban, A. L.; Díez, E.; Head, N. J.; Della, E. W. *Mol. Phys.* **2006**, *104*, 485.

(4) (a) dos Santos, F. P.; Tormena, C. F.; Contreras, R. H.; Rittner, R.; Magalhães, A. *Magn. Reson. Chem.* **2008**, *46*, 107. (b) Pérez, C.; Suardíaz, R.; Ortiz, P. J.; Crespo-Otero, R.; Bonetto, G. M.; Gavín, J. A.; García de la Vega, J. M.; SanFabián, J.; Contreras, R. H. *Magn. Reson. Chem.* **2008**, *46*, 846. (c) Contreras, R. H.; Suardíaz, R.; Pérez, C.; Crespo-Otero, R.; SanFabián, J.; García de la Vega, J. M. *J. Chem. Theory Comput.* **2008**, *4*, 1494. (d) Gauze, G. F.; Basso, E. A.; Contreras, R. H.; Tormena, C. F. *J. Phys. Chem. A* **2009**, *113*, 2647.

(5) (a) Reed, A. E.; Curtiss, L. A.; Weinhold, F. *Chem. Rev.* **1988**, *88*, 899. (b) Weinhold, F. In *Encyclopedia of Computational Chemistry*; Schleyer, P. v. R., Ed.; Wiley: New York, 1998; Vol. 3, p 1792.

(6) Glendening, E. D.; Badenhoop, J. K.; Reed, A. E.; Carpenter, J. E.; Bohmann, J. A.; Morales, C. M.; Weinhold, F. *NBO 5.0.*; Theoretical Chemistry Institute, University of Wisconsin: Madison, WI, 2001.

(7) (a) Diz, A. C.; Contreras, R. H.; Natiello, M. A.; Gavarini, H. O. *J. Comput. Chem.* **1985**, *6*, 647. (b) Giribet, C. G.; Ruiz de Azúa, M. C.; Contreras, R. H.; Lobayan de Bonczok, R.; Aucar, G. A.; Gómez, S. *J. Mol. Struct.* **1993**, *300*, 467.

(8) Engelmann, A. R.; Contreras, R. H. *Int. J. Quantum Chem.* **1983**, *23*, 1033.

(9) Malkina, O. L.; Malkin, V. G. *Angew. Chem., Int. Ed.* **2003**, *42*, 4335.

(10) Petzold, H.; Gorls, H.; Weigand, W. *J. Organomet. Chem.* **2007**, *692*, 2736.

(11) (a) Carty, A. J.; Johnson, D. K.; Jacobson, S. E. *J. Am. Chem. Soc.* **1979**, *101*, 5612. (b) Grim, S. O.; Smith, P. H.; Colquhoun, I. J.; McFarlane, W. *Inorg. Chem.* **1980**, *19*, 3195. (c) McFarlane, H. C. E.; McFarlane, W. *Polyhedron* **1999**, *18*, 2117. (d) Karaçara, A.; Freytaga, M.; Thönnessena, H.; Omelanczukb, J.; Jonesa, P. G.; Bartscha, R.; Schmutzler, R. Z. *Anorg. Allg. Chem.* **2000**, *626*, 2361. (e) Ganesamoorthy, C.; Balakrishna, M. S.; Mague, J. T.; Tuononen, H. M. *Inorg. Chem.* **2008**, *47*, 7035.

(12) (a) Hierso, J.-C.; Evrard, D.; Lucas, D.; Richard, P.; Cattey, H.; Hanquet, B.; Meunier, P. *J. Organomet. Chem.* **2008**, *693*, 574. (b) Beaupérin, M.; Fayad, E.; Amardeil, R.; Cattey, H.; Richard, P.; Brandès, S.; Meunier, P.; Hierso, J. -C. *Organometallics* **2008**, *27*, 1506. (c) Thomas, D. A.; Ivanov, V. V.; Butler, I. R.; Horton, P. N.; Meunier, P.; Hierso, J. -C. *Inorg. Chem.* **2008**, *47*, 1607. (d) Smaliy, R. V.; Beaupérin, M.; Cattey, H.; Meunier, P.; Hierso, J. -C. *Organometallics* **2009**, *28*, 3152.

(13) (a) Zschynke, A.; Mügge, C.; Meyer, H.; Jurkschat, K. *Org. Magn. Reson.* **1983**, *21*, 315. (b) Quin, L. D. *The Heterocyclic Chemistry of Phosphorus*; Wiley Interscience: New York, 1981. (c) Gorenstein, D. G. *Prog. NMR Spectrosc.* **1983**, *16*, 1. (d) Ebsworth, E. A. V.; Rankin, D. W. H.; Wright, J. G. *J. Chem. Soc., Dalton Trans.* **1979**, 1065. (e) Gavarini, H. O.; Natiello, M. A.; Contreras, R. H. *Theor. Chim. Acta* **1985**, *68*, 171.

(14) (a) Contreras, R. H.; Peralta, J. E. *Prog. NMR Spectrosc.* **2000**, *37*, 321. (b) Contreras, R. H.; Barone, V.; Facelli, J. C.; Peralta, J. E. *Annu. Rep. NMR Spectrosc.* **2003**, *51*, 167.

(15) (a) Oddershede, J. Polarization Propagator Calculations. In *Advances in Quantum Chemistry*; Löwdin, P.-O., Ed.; Academic Press: New York, 1978; Vol. 11, p 275. (b) Diz, A. C.; Giribet, C. G.; Ruizde Azúa, M. C.; Contreras, R. H *Int. J. Quantum Chem.* **1990**, *37*, 663. (c) Contreras, R. H.; Ruiz de Azúa, M. C.; Giribet, C. G.; Aucar, G. A.; Lobayan de Bonczok, R. *J. Mol. Struct. (THEOCHEM)* **1993**, *284*, 249.

(16) (a) Ruiz de Azúa, M. C.; Giribet, C. G.; Vizioli, C. V.; Contreras, R. H. *J. Mol. Struct. (THEOCHEM)* **1998**, *433*, 141. (b) Giribet, C. G.; Ruiz de Azúa, M. C. *J. Phys. Chem. A* **2005**, *109*, 11980. (c) Giribet, C. G.; Ruiz de Azúa, M. C. *J. Phys. Chem. A* **2006**, *110*, 11575. (d) Giribet, C. G.; Ruiz de Azúa, M. C. *J. Phys. Chem A* **2008**, *112*, 4386.

(17) Kohn, W.; Sham, L. J. *Phys. Rev. A* **1965**, *140*, 1133.

(18) Cremer, D.; Gräfenstein, J. *Phys. Chem. Chem. Phys.* **2007**, *9*, 2791, and references cited therein. .

(19) Provasi, P. F.; Sauer, S. P. A. *Phys. Chem. Chem. Phys.* **2009**, *11*, 3987.

(20) (a) Contreras, R. H.; Esteban, A. L.; Díez, E.; Della, E. W.; Lochert, I. J.; dos Santos, F. P.; Tormena, C. F. *J. Phys. Chem., A* **2006**, *110*, 4266. (b) Contreras, R. H.; Esteban, A. L.; Díez, E.; Lochert, I. J.; Della, E. W.; Tormena, C. F. *Magn. Reson. Chem.* **2007**, *45*, 572. (c) Cunha Neto, A.; dos Santos, F. P.; Contreras, R. H.; Rittner, R.; Tormena, C. F. *J. Phys. Chem. A* **2008**, *112*, 11956.

(21) Krivdin, L. B.; Contreras, R. H. *Annu. Rep. NMR Spectrosc.* **2007**, *61*, 133.

(22) Frisch, M. J.; Trucks, G. W.; Schlegel, H. B.; Scuseria, G. E.; Robb, M. A.; Cheeseman, J. R.; Montgomery, J. A., Jr.; Vreven, T.; Kudin, K. N.; Burant, J. C.; Millam, J. M.; Iyengar, S. S.; Tomasi, J.; Barone, V.; Mennucci, B.; Cossi, M.; Scalmani, G.; Rega, N.; Petersson, G. A.; Nakatsuji, H.; Hada, M.; Ehara, M.; Toyota, K.; Fukuda, R.; Hasegawa, J.; Ishida, M.; Nakajima, T.; Honda, Y.; Kitao, O.; Nakai, H.; Klene, M.; Li, X.; Knox, J. E.; Hratchian, H. P.; Cross, J. B.; Bakken, V.; Adamo, C.; Jaramillo, J.; Gomperts, R.; Stratmann, R. E.; Yazyev, O.; Austin, A. J.; Cammi, R.; Pomelli, C.; Ochterski, J. W.; Ayala, P. Y.; Morokuma, K.; Voth, G. A.; Salvador, P.; Dannenberg, J. J.; Zakrzewski, V. G.; Dapprich, S.; Daniels, A. D.; Strain, M. C.; Farkas, O.; Malick, D. K.; Rabuck, A. D.; Raghavachari, K.; Foresman, J. B.; Ortiz, J. V.; Cui, Q.; Baboul, A. G.; Clifford, S.; Cioslowski, J.; Stefanov, B. B.; Liu, G.; Liashenko, A.; Piskorz, P.; Komaromi, I.; Martin, R. L.; Fox, D. J.; Keith, T.; Al-Laham, M. A.; Peng, C. Y.; Nanayakkara, A.; Challacombe, M.; Gill, P. M. W.; Johnson, B.; Chen, W.; Wong, M. W.; Gonzalez, C.; Pople, J. A. *Gaussian 03*, revision E.01; Gaussian: Wallingford, CT, 2004.

(23) Møller, C.; Plesset, M. S. *Phys. Rev.* **1934**, *46*, 618.

(24) Dunning, T. H.; Peterson, K. A.; Wonn, D. E. In *Encyclopedia of Computational Chemistry*; Wiley: New York, 1998; Vol. 1, p 88.

(25) (a) Becke, A. D. *Phys. Rev. A* **1988**, *38*, 3098. (b) Becke, A. D. *J. Chem. Phys.* **1993**, *98*, 5648. (c) Lee, C. T.; Yang, W. T.; Parr, R. G. *Phys. Rev. B* **1988**, *37*, 785.

(26) Kutzelnigg, W.; Fleischer, U.; Schindler, M. The IGLO-Method: Ab-Initio Calculation and Interpretation of NMR Chemical Shifts and Magnetic Susceptibilities. In *NMR Basic Principles and Progress*; Springer-Verlag: Berlin, 1990; Vol. 23, pp 165−262.

(27) Sychrovshý, V.; Gräfenstein, J.; Cremer, D. *J. Chem. Phys.* **2000**, *113*, 3530.

(28) Jensen, F. *J. Chem. Theory Comput.* **2006**, *2*, 1360.

(29) Carty, A. J.; Johnson, D. K.; Jacobson, S. E. *J. Am. Chem. Soc.* **1979**, *101*, 5612.

(30) Rudolph, R. W.; Newmark, R. A. *J. Am. Chem. Soc.* **1970**, *92*, 1195.

JP908970F